# Auger-electron emission from collisionally excited 3.4-MeV/u Na-like Ti ions

D. Schneider, P. Beiersdorfer, M. Chen, R. Walling, J. D. Molitoris, and D. De Witt
*Department of Physics, V-Division, University of California, Lawrence Livermore National Laboratory, Livermore, California 94550*
(Received 18 January 1989)

*L* Auger-electron emission following selective excitation of autoionizing states in 3.4-MeV/u Na-like Ti ions by He and Ar has been investigated using the technique of 0° electron spectroscopy. The electron emission has been compared to model spectra based on oscillator strengths, transition energies, and transition rates from multiconfigurational Dirac-Fock calculations as well as on collision strengths from the literature. It was found that monopole, dipole, and quadrupole excitation of Auger states with an excited-state configuration $2p^5 3snl$ ($n=3,4$) causes the dominating structure in the spectrum where He was used as an exciter.

## I. INTRODUCTION

Nonradiative decay studies of collisionally excited fast-beam ions have been performed on ions ranging from He to Ar over the past two decades (e.g., Refs. 1–5). In the early experiments the emission of Auger electrons following the deexcitation of foil- or gas-target excited projectile ions has been measured at small forward angles. These investigations were extended through the technique of 0° Auger-electron spectroscopy,[6,7] where the various kinematic advantages, in particular, make it possible to perform Auger-electron spectroscopy with very-high-energy resolution [$<0.1\%$ full width at half maximum (FWHM)].[8] Moreover, the investigation of Auger decay in highly stripped ions was aided by employing the method of selective ionization of fast ions in collisions with He.[6,9] The particular advantages of the selective ionization method using fast beams and light target atoms in ion-atom collisions has been outlined in Refs. 5, 6, 8, and 9. The success of this method is partly due to the ability to select specific charge states prior to collisional excitation. This can be achieved readily by charge analyzing, and by selecting highly stripped fast ions from high-energy accelerators.

The spectroscopy of secondary electrons (e.g., Auger electrons) performed in energetic ion-atom collisions, provides not only atomic structure data, it also provides insight into the dynamics of excitation and deexcitation mechanisms in highly ionized ions. It thus provides valuable information which complements photon emission spectroscopy. Furthermore, the spectroscopy of electrons provides a most significant tool for understanding the dynamics of atomic collision processes.

In this paper we have studied the 0° Auger spectra of Na-like Ti ions excited by collisions with He and Ar target gases. We have attempted to understand the dynamics of the excitation mechanism by modeling the observed Auger spectra using results from multiconfigurational Dirac-Fock (MCDF) atomic structure calculations and excitation rates provided in the literature. Good agreement between the model calculations and the data is obtained. The model calculations show that dipole-forbidden excitations play a significant role in populating excited levels. Dipole-forbidden excitations are predicted to be a dominant population mechanism for creating population inversions in collisionally pumped x-ray laser schemes.[10] The present observations represent a measurement of the relative magnitude of this mechanism in Na-like ions.

Previous investigations of *L* Auger-electron emission have been performed for highly charged Na- and Mg-like ions with an atomic number as large as $Z=18$ (argon). The present results are the first data for fast highly charged higher-$Z$ ions. Complementary investigations using slow highly charged ions are presently performed using the electron cyclotron resonance source at the Lawrence Berkeley Laboratory.[11]

## II. EXPERIMENTAL ARRANGEMENT

High-quality beams of 3.4 MeV/u $Ti^{+11}$ were provided by the Lawrence Berkeley Laboratory Super-HILAC. The experimental setup used to perform 0° Auger-electron spectroscopy is similar to the setup described in Ref. 2. A schematic of the setup is given in Fig. 1. The incident ion beam is tightly collimated through two four-jaw entrance collimators to a spot size of about 2 $mm^2$. The average beam intensity ranged from 1 to 3 electrical nA. The gas cell employed was 12 cm in length and was maintained at a constant pressure of 6.0 Torr, which guarantees single-collision conditions. The exit of the gas cell was 1.7 cm from the entrance of a set of 45° parallel-plate electrostatic deflectors which comprise the first stage of a tandem 0° electron spectrometer developed at the Hahn-Meitner-Institut in Berlin. The first stage serves to deflect the electrons while the heavy-ion projectiles pass through slits in the deflector and are collected downstream in a Faraday cup. The second stage of the spectrometer energy analyzes the electrons with high-energy resolution. The electrons are then counted by a microchannel plate at the exit of the spectrometer. The energy resolution of the present setup is 7.5% FWHM; the solid angle is about $10^{-4}$ sr.

Figure 2(a) shows a typical spectrum over the complete scanning range of the spectrometer. The pronounced "cusp" peak in the spectrum arises from electrons traveling with the beam velocity. The origin of the cusp peak

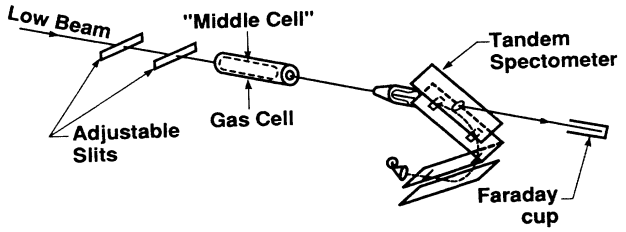


FIG. 1. Schematic of the experimental setup to perform 0° Auger-electron spectroscopy at the Lawrence Berkeley Laboratory Super-HILAC accelerator. The setup is similar to the one described in Ref. 2.

is well known; it arises from electron capture and/or loss to projectile centered continuum states.[8,9]

For the present study the most significant aspect of Fig. 2(a) is the structure due to $L$ Auger-electron emission of Ti which is shifted to higher and lower energies in relation to the cusp. The electron energy of the cusp peak maximum is equivalent to the projectile energy reduced by the projectile mass to electron mass ratio. The energy of the cusp serves as an energy calibration for the projectile energy which is used to transform the energies and intensities of the Ti $L$ Auger peaks into emitter rest frame energies. In turn, matching of the Ti $L$ Auger energies observed at lower and higher electron laboratory energies with respect to the cusp peak after the transformation allows us to determine the projectile energy within the given electron energy resolution. This is demonstrated in Fig. 2(b). Although the structure at lower electron energies is taken with poor statistics, the projectile energy and therefore the Auger peak energy can be given within an accuracy of $\pm 7.5\%$ according to the electron spectrometer's intrinsic resolution of 7.5% (FWHM).

## III. COMPARISON WITH THE MODEL CALCULATIONS

The Auger-electron spectra after background subtraction and transformation into the emitter rest frame are shown in Fig. 3. The figure shows that the spectra produced by collisions with He and Ar, respectively, are very similar except for the relative cross-section increase when going from the He to the Ar target. The structure of both spectra is similar, and peak electron emission occurs in both at the same energy of about 227 eV. The major difference between the two spectra is that relative to the respective peak intensities a higher electron emission in the energy ranges 240–320 and 400–500 eV is observed in the Ar-target spectrum than in the He-target spectrum.

In order to understand the Auger spectra we have developed a simple model based on collisional excitation of ions in the ground state to autoionizing states and subsequent decay. The model makes use of the property of selective excitation in which light target atoms such as He selectively excite inner-shell electrons of the projectile ions without disturbing outer-shell electrons [a property referred to as "needle" excitation (ionization)].[6] For the

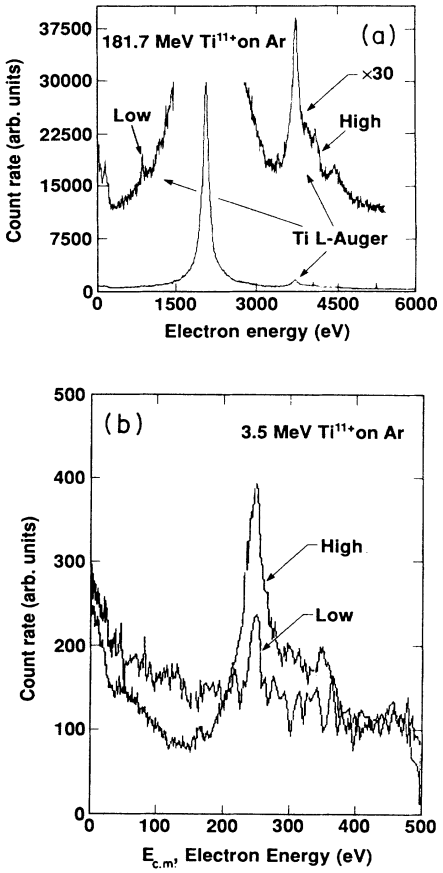


FIG. 2. (a) Total electron spectra obtained from collisions of 181.7 MeV $Ti^{11+}$ with Ar. The spectrum in (b) shows the peak intensities due to Ti $L$ Auger electrons after transformation into rest-frame energies from intensities at the low-energy side of the cusp peak and high-energy side, respectively.

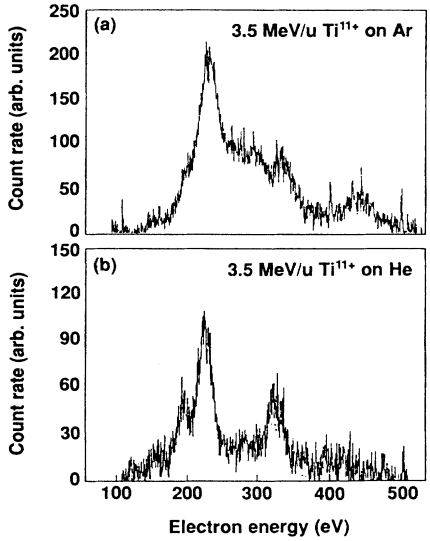


FIG. 3. Ti $L$ Auger-electron spectra observed at the high-energy side of the cusp peak resulting from the collisions of 181.7 MeV $Ti^{11+}$ (a) with He and (b) with Ar. The intensities are plotted vs rest-frame energies after background subtraction.

TABLE I. Spectroscopic data for $3s3l$ Auger lines in $Ti^{11+}$ excited by dipole excitation from the ground state and decaying to the $2s^22p^6\,{}^1S_0$ neonlike ground state. $J$ is the total angular momentum of the upper level; $E_{Au}$ is the energy of the Auger electron; $A^a$ is the autoionization rate, $\beta$ is the branching ratio for autoionization; and $I$ is the relative intensity of each line according to Eq. (1) normalized to the strongest line at $E_{Au}=228.37$ eV. Only lines with $I \geq 0.03$ are listed.

| Upper level | $J$ | $E_{Au}$ (eV) | $A^a$ ($sec^{-1}$) | $\beta$ | $I$ |
|---|---|---|---|---|---|
| $2s^22p^5_{3/2}3s^2$ | 1.5 | 157.48 | 2.08+12 | 0.89 | 0.11 |
| $2s^22p^5_{1/2}3s^2$ | 0.5 | 163.24 | 2.03+12 | 0.89 | 0.06 |
| $2s2p^5_{3/2}3s_{1/2}3d_{5/2}$ | 1.5 | 221.32 | 1.55+13 | 0.94 | 0.26 |
| $2s^22p^5_{3/2}3s_{1/2}3d_{5/2}$ | 0.5 | 221.41 | 2.70+13 | 0.96 | 0.16 |
| $2s^22p^5_{1/2}3s_{1/2}3d_{3/2}$ | 1.5 | 224.16 | 3.97+13 | 0.99 | 0.03 |
| $2s^22p^5_{1/2}3s_{1/2}3d_{3/2}$ | 0.5 | 227.86 | 2.63+14 | 0.99 | 0.20 |
| $2s^22p^5_{1/2}3s_{1/2}3d_{3/2}$ | 1.5 | 228.37 | 2.45+14 | 0.99 | 1.00 |
| $2s^22p^5_{3/2}3s_{1/2}3d_{5/2}$ | 1.5 | 230.94 | 1.20+13 | 0.80 | 0.74 |
| $2s^22p^5_{3/2}3s_{1/2}3d_{5/2}$ | 0.5 | 232.65 | 1.39+13 | 0.63 | 0.82 |
| $2s^22p^5_{1/2}3s_{1/2}3d_{5/2}$ | 1.5 | 235.99 | 3.61+13 | 0.91 | 0.99 |
| $2s2p^63s_{1/2}3p_{1/2}$ | 0.5 | 289.25 | 6.82+13 | 0.99 | 0.11 |
| $2s^22p^5_{1/2}3s_{1/2}3d_{5/2}$ | 1.5 | 289.64 | 1.59+13 | 0.98 | 0.04 |
| $2s2p^63s_{1/2}3p_{3/2}$ | 1.5 | 289.99 | 4.28+13 | 0.98 | 0.19 |

projectile energy in the present experiment we expect collisions to result in the excitation of a single $2s$ or $2p$ inner-shell electron and thus to product autoionizing configurations of the type $1s^22s2p^63snl$ or $1s^22s^22p^53snl$, where $n \geq 3$. As a result, the population density of a given autoionizing level $j$ is related to the excitation cross section $\sigma_{gj}$ from the ground state. In the Bethe approximation for dipole-allowed excitation, $\sigma_{gj}$ can be expressed in terms of the absorption oscillator strength $f_{gj}$ and the excitation energy $E_{gj}$, i.e., $\sigma_{gj} \propto f_{gj}/E_{gj}$.[12] Therefore, we have modeled the intensity $I_j$ of the electron line emission resulting from Auger decay of level $j$ as

$$I_j = K_1 \beta_j f_{gj}/E_{gj} \ . \quad (1)$$

Here $\beta_j$ is the branching ratio for Auger decay of level $j$, i.e., $\beta_j = A^a_j/(A^a_j + A^r_j)$, where $A^a_j$ is the Auger decay rate and the $A^r_j$ is the radiative decay rate to the ground state. Radiative decay branches other than the x-ray branch have not been included, because rates of intrashell transitions are typically negligibly small compared to the dipole-allowed x-ray branch. Because of this, the effect of cascades has also been neglected in our model. The constant $K_1$ is chosen so that the intensity of the strongest line equals unity.

A summary of the Auger transitions predicted with the help of Eq. (1) is given in Tables I and II. The tables include transitions from autoionizing configurations $3snl$

TABLE II. Spectroscopic data for $3s4l$ Auger lines in $Ti^{11+}$ excited by dipole excitation from the ground state and decaying to the $2s^22p^6\,{}^1S_0$ neonlike ground state. $J$ is the total angular momentum of the upper level; $E_{Au}$ is the energy of the Auger electron; $A^a$ is the autoionization rate; $\beta$ is the branching ratio for autoionization; and $I$ is the relative intensity of each line according to Eq. (1) normalized to the strongest Auger line in Table I. $I^*$ represents the relative intensity used in the fit of the spectrum in Fig. 4. Only lines with $I^* \geq 0.03$ are listed.

| Upper level | $J$ | $E_{Au}$ (eV) | $A^a$ ($sec^{-1}$) | $\beta$ | $I$ | $I^*$ |
|---|---|---|---|---|---|---|
| $2s^22p^5_{3/2}3s_{1/2}4d_{5/2}$ | 1.5 | 326.38 | 6.54+11 | 0.79 | 0.017 | 0.08 |
| $2s^22p^5_{3/2}3s_{5/2}4d_{3/2}$ | 0.5 | 326.44 | 3.21+12 | 0.91 | 0.009 | 0.04 |
| $2s^22p^5_{3/2}3s_{5/2}4d_{3/2}$ | 1.5 | 326.79 | 1.89+12 | 0.87 | 0.010 | 0.05 |
| $2s^22p^5_{3/2}3s_{1/2}4d_{5/2}$ | 0.5 | 327.45 | 3.30+12 | 0.78 | 0.072 | 0.32 |
| $2s^22p^5_{3/2}3s_{1/2}4d_{5/2}$ | 1.5 | 328.46 | 1.61+12 | 0.59 | 0.104 | 0.47 |
| $2s^22p^5_{1/2}3s_{1/2}4d_{3/2}$ | 1.5 | 331.27 | 8.88+11 | 0.81 | 0.023 | 0.10 |
| $2s^22p^5_{1/2}3s_{1/2}4d_{3/2}$ | 1.5 | 333.05 | 1.61+12 | 0.56 | 0.107 | 0.48 |
| $2s^22p^5_{1/2}3s_{1/2}4d_{3/2}$ | 0.5 | 333.23 | 1.82+12 | 0.55 | 0.065 | 0.29 |
| $2s^22p^5_{3/2}3p_{3/2}4p_{3/2}$ | 1.5 | 336.56 | 2.78+11 | 0.71 | 0.015 | 0.07 |
| $2s^22p^5_{3/2}3p_{1/2}4p_{3/2}$ | 0.5 | 337.47 | 1.28+12 | 0.90 | 0.011 | 0.05 |
| $2s2p^63s_{1/2}4p_{1/2}$ | 0.5 | 424.01 | 3.68+13 | 0.99 | 0.014 | 0.06 |
| $2s2p^63s_{1/2}4p_{3/2}$ | 1.5 | 424.42 | 3.81+13 | 0.99 | 0.026 | 0.12 |

with $n=3$ or $n=4$, respectively. The Auger energies have been calculated using a MCDF program.[13] The program has also provided the corresponding Auger rates and oscillator strengths as well as radiative rates for electric dipole decay to the $1s^2 2s^2 2p^6 3s$ ground state.

So far we have only considered dipole-allowed excitations for populating excited levels. However, observations of x-ray transitions in high-$Z$ Na-, Mg-, F-, and Ne-like ions have shown that dipole-forbidden excitations play a major role in populating excited states.[14,15] In Ne-like ions, for example, observations of the x-ray emission from low-density plasmas indicates that levels of the type $(1s^2 2s^2 2p^5 3p)_{J=2}$ and $(1s^2 2s 2p^6 3d)_{J=2}$ are populated by $\Delta J=2$ dipole-forbidden collisions from the ground state.[14] These levels form the upper states in collisionally pumped x-ray lasing schemes.[10] Moreover, $\Delta J=0$ dipole-forbidden excitation from the ground state to levels of the type $(1s^2 s^2 2p^5 3p)_{J=0}$ is also predicted to play a major role in collisionally pumped x-ray lasing schemes.[10] Therefore, we expect that dipole-forbidden excitations significantly contribute to line emission in our Auger spectra. The Auger line emission due to dipole-forbidden excitations from the ground state is modeled as

$$I_j = K_2 \beta_j \Omega_{gj} \ . \tag{2}$$

Here $\Omega_{gj}$ represents the collision strength for the excitation of level $j$ from the ground state. Its values have been calculated by Zhang and Sampson.[16] The constant $K_2$ is chosen so as to normalize the intensities computed from Eq. (2) to the intensities of dipole-allowed transitions computed from Eq. (1).

A summary of Auger line intensities excited by dipole-forbidden collisional excitation is given in Table III for configurations $3s3l$. The Auger energies as well as the corresponding Auger and radiative rates are again from our MCDF calculations. The radiative rates used in the Auger branching ratio $\beta$ are $\Delta n=1$ electric dipole decay rates to lower levels of the type $1s^2 2s^2 2p^6 3l$.

The atomic data and intensity information in Tables I–III has been used to fit the $Ti^{11+}$ $L$ Auger spectrum produced in collisions with He. The result is shown in Fig. 4(a). A spectral resolution of $\Delta E/E=0.075$ was assumed in the theoretical spectrum to allow for summation of close by Auger transitions. It was necessary to shift the theoretical spectrum as a whole by about $-4$ eV, i.e., the calculated Auger energies were generally 4 eV larger than measured. The spectral regions near 100 and 500 eV are used to determine the offset of the experimental data. The intensity of the model spectrum has been adjusted until the best fit to the experimental spectrum was achieved. The best fit is obtained if the contributions from the decay of the $n=3$ dipole-allowed, of the $n=3$ dipole-forbidden, and of the $n=4$ dipole-allowed levels each are varied separately. The separate contributions from each of the three groups of levels are shown in Figs. 4(b)–4(d).

The relative intensities of the Auger lines resulting from dipole-allowed and dipole-forbidden excitations of inner-shell electrons to the $n=3$, 4 shells used in the fit are given in Tables I–III. Best fit to the peaks at 190 and 230 eV is achieved if the relative intensities of the dipole-forbidden lines are enhanced by about 16% over the values computed by Eq. (2). By contrast, a good fit of the peak at 330 eV can only be obtained if the relative intensity of the Auger lines resulting from dipole-allowed excitation of inner-shell electrons to the $n=4$ shell is increased by a factor of 4.5 over the values computed by Eq. (1). Alternatively, we could have fitted the peak at 330 eV by increasing the contribution of the dipole-forbidden levels. This possibility is suggested by Fig. 4(c). However, this would entail an increase of the intensity of these Auger lines by a factor of 5 and would destroy the good fit of the peak at 190 eV.

The theoretical spectrum shown in Fig. 4 matches the experimental spectrum well. This indicates that the model is appropriate for the analysis of the Auger spectra induced by fast ions colliding with low-$Z$ target gases. Fu-

TABLE III. Spectroscopic data for $3s3l$ Auger lines in $Ti^{11+}$ excited by dipole-forbidden excitation from the ground state and decay to the $2s^2 2p^6\,{}^1S_0$ neonlike ground state. $J$ is the total angular momentum of the upper level; $E_{Au}$ is the energy of the Auger electron; $A^a$ is the autoionization rate; $\beta$ is the branching ratio for autoionization; and $I$ is the relative intensity of each line according to Eq. (2) normalized to the strongest Auger line in Table I. $I^*$ represents the relative intensity used in the fit of the spectrum in Fig. 4. Only lines with $I^* \geq 0.03$ are listed.

| Upper level | $J$ | $E_{Au}$ (eV) | $A^a$ ($sec^{-1}$) | $\beta$ | $I$ | $I^*$ |
|---|---|---|---|---|---|---|
| $2s^2 2p^5_{1/2} 3s_{1/2} 3p_{3/2}$ | 0.5 | 195.14 | 1.71+13 | 0.98 | 0.11 | 0.13 |
| $2s^2 p^5_{3/2} 3s_{1/2} 3p_{3/2}$ | 0.5 | 202.43 | 3.67+14 | 1.00 | 1.00 | 1.16 |
| $2s^2 2p^5_{1/2} 3s_{1/2} 3d_{5/2}$ | 3.5 | 224.77 | 1.07+12 | 0.85 | 0.03 | 0.03 |
| $2s2p^6 3s^2$ | 0.5 | 265.83 | 2.51+13 | 1.00 | 0.18 | 0.21 |
| $2s2p^6 3s_{1/2} 3d_{3/2}$ | 1.5 | 329.20 | 3.25+13 | 1.00 | 0.16 | 0.18 |
| $2s2p^6 3s_{1/2} 3d_{5/2}$ | 2.5 | 329.28 | 3.13+13 | 1.00 | 0.24 | 0.28 |
| $2s2p^6 3s_{1/2} 3d_{3/2}$ | 2.5 | 335.03 | 5.00+13 | 1.00 | 0.03 | 0.03 |
| $2s2p^6 3s_{1/2} 3d_{5/2}$ | 1.5 | 335.03 | 4.97+13 | 1.00 | 0.03 | 0.03 |

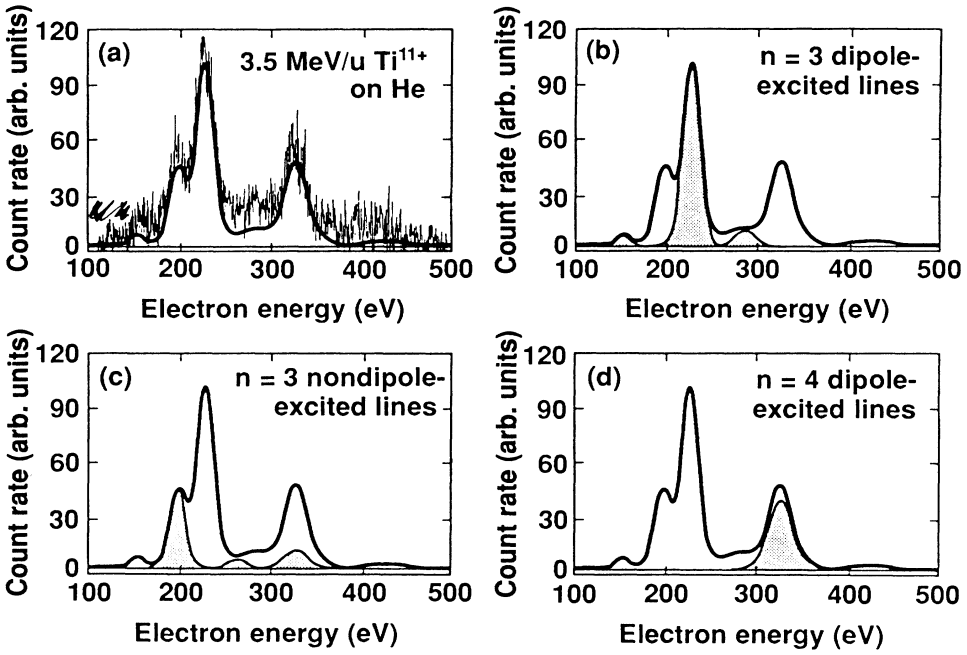


FIG. 4. Comparison of measured $Ti^{11+}$ $L$ Auger-electron intensities [Fig. 3(b)] with a model spectrum described in the text. Individual contributions to the model spectrum are shown in (b)–(d).

ture models may need to include levels with electrons in the $n=4$ shell excited by dipole-forbidden transitions, or configuration $3snl$ with $n \geq 5$. This, however, does not seem necessary for modeling the present spectrum.

In the Auger spectrum resulting from collisions with Ar, Fig. 3(b), features similar to those in the He-target spectrum can be identified. In addition, however, the spectrum shows increased line intensities in the energy range 250–310 eV, and a pronounced peak at 440 eV. Since Ar is a much heavier element than He, we expect additional processes to populate autoionizing states besides needle excitation. For example, a collision may not only result in the excitation of an inner-shell electron, but the $3s$ outer-shell electron may be excited as well. The possibility of electron capture is also greatly enhanced for high-$Z$ gases due to velocity matching of bound target electron with the projectile velocity. These processes may also be weakly present in collisions with the He target as suggested by the observed intensities in the energy ranges 250–310 and 380–420 eV not accounted for by the model spectrum. The modeling of these processes has been left for future efforts.

## IV. CONCLUSION

We measured $L$ Auger spectra following the excitation of 3.4 MeV/u $Ti^{11+}$ ions in He and Ar gas targets. The dominant structure observed in the spectrum following excitation with He results from monopole, dipole, and quadrupole excitation of the $2s^22p^63s$ ground-state configuration into $2s^22p^53snl$ excited-state configurations. The different states that can contribute to the unresolved peak structure are assigned. The most probable excited level is the $(2s^22p^5_{3/2}3s\,3p_{3/2})_{J=1/2}$ level populated by monopole excitation. It was found by comparison to oscillator strengths that higher-order excitation modes contribute to the observed peak structure; this is found to be enhanced in the case where Ar is used as an exciter.

## ACKNOWLEDGMENTS

This work was performed under the auspices of the U. S. Department of Energy by Lawrence Livermore National Laboratory under Contract No. W-7405-ENG-48.

[1]S. Schumann, K. O. Groeneveld, G. Nolte, and B. Fricke, Z. Phys. A **280**, 245 (1979).

[2]D. Schneider, R. Bruch, W. H. E. Schwartz, T. C. Cheng, K. T. Cheng, and C. F. Moore, Phys. Rev. A **15**, 926 (1977); R. Bruch, D. Schneider, W. H. E. Schwartz, M. Meinhart, B. M. Johnson, and K. Taulbjerg, *ibid.* **19**, 587 (1979).

[3]H. H. Haselton, R. S. Thoe, J. R. Mowat, P. M. Griffin, D. J. Pegg, and I. A. Sellin, Phys. Rev. A **11**, 468 (1975).

[4]R. Bruch, M. Rodbro, P. Bisgaard, and P. Dahl, Phys. Rev. Lett. **39**, 801 (1977).

[5]D. Schneider, W. Hodge, B. M. Johnson, L. E. Smith, and C. F. Moore, Phys. Lett. A **54**, 174 (1975).

[6]A. Itoh, T. Schneider, G. Schiwietz, Z. Roller, H. Platten, G. Nolte, D. Schneider, and N. Stolterfoht, J. Phys. B **16**, 3965

(1983).

[7]A. Itoh, D. Schneider, T. Schneider, T. Zouros, G. Nolte, G. Schiwietz, W. Zeitz, and N. Stolterfoht, Phys. Rev. A **31**, 684 (1985).

[8]N. Stolterfoht, A. Itoh, D. Schneider, T. Schneider, G. Schiwietz, H. Platten, G. Nolte, R. Glodde, U. Stettner, W. Zeitz, and T. Zouros, Invited Lecture, *International Conference on X-ray and Inner Shell Processes in Atoms, Molecules and Solids,* Leipzig, GDR, 1985.

[9]D. Schneider, N. Stolterfoht, G. Schiwietz, T. Schneider, W. Zeitz, R. Bruch, and K. T. Cheng, Nucl. Instrum. Methods B **24**, 173 (1987).

[10]M. D. Rosen *et al.,* Phys. Rev. Lett. **54**, 106 (1985); D. L. Matthews *et al., ibid.* **54**, 110 (1985).

[11]D. Schneider, R. Hutton, and M. Prior, Auger Electron Spectroscopy on High $Z$ Na-like Ions, Proceedings of the Symposium on the Auger Effect, Paris, 1989.

[12]I. I. Sobelman, L. A. Vainshtein, and E. A. Yukov, *Excitation of Atoms and Broadening of Spectral Lines* (Springer-Verlag, Berlin, 1981), p. 41.

[13]I. P. Grant, B. J. McKenzie, P. H. Norrington, D. F. Mayers, and N. C. Pyper, Comput. Phys. Commun. **21**, 207 (1980).

[14]D. D. Dietrich, G. A. Chandler, R. J. Fortner, C. J. Hailey, and R. E. Stewart, Phys. Rev. Lett. **54**, 1008 (1985).

[15]P. Beiersdorfer, M. Bitter, S. von Goeler, S. Cohen, K. W. Hill, J. Timberlake, R. S. Walling, M. H. Chen, P. L. Hagelstein, and J. H. Scofield, Phys. Rev. A **34**, 1297 (1986); P. Beiersdorfer, *et al., ibid* **37**, 4153 (1988).

[16]H. Zhang and D. H. Sampson, At. Data Nucl. Data Tables (unpublished).